Smart Structures and Systems, Vol. 9, No. 2 (2012) 105-125
DOI: http://dx.doi.org/10.12989/sss.2012.9.2.105

Exact solutions of free vibration of rotating multilayered FGM cylinders

Chih-Ping Wu* and Hao-Yuan Li

Department of Civil Engineering, National Cheng Kung University, Tainan 70101, Taiwan, ROC

(Received March 28, 2011, Revised January 11, 2012, Accepted January 13, 2012)

Abstract. A modified Pagano method is developed for the three-dimensional (3D) free vibration analysis of simply-supported, multilayered functionally graded material (FGM) circular hollow cylinders with a constant rotational speed with respect to the meridional direction of the cylinders. The material properties of each FGM layer constituting the cylinders are regarded as heterogeneous through the thickness coordinate, and then specified to obey a power-law distribution of the volume fractions of the constituents, and the effects of centrifugal and Coriolis accelerations, as well as the initial hoop stress due to rotation, are considered. The Pagano method, which was developed for the static and dynamic analyses of multilayered composite plates, is modified in that a displacement-based formulation is replaced by a mixed formulation, the complex-valued solutions of the system equations are transferred to the real-valued solutions, a successive approximation method is adopted to extend its application to FGM cylinders, and a propagator matrix method is developed to reduce the time needed for its implementation. These modifications make the Pagano method feasible for multilayered FGM cylinders, and the computation in the implementation is independent of the total number of the layers, thus becoming less time-consuming than usual.

Keywords: Pagano method; vibration; rotating cylinders; Coriolis acceleration; functionally graded material.

1. Introduction

The dynamic responses of rotating and non-rotating circular hollow cylinders, which are made up of homogeneous isotropic, composite and functionally graded materials (FGMs), has attracted considerable research attention as these cylinders have a wide range of applications, and are increasingly being used in advanced technologies, such as high-speed centrifugal separators, high-power aircraft jet engines, locomotive engines, drive shafts of gas turbines, certain motor and rotor systems, and rotating magnetic shields.

In 1890, Bryan (1890) first studied the dynamic responses of a rotating isotropic cylinder and found the traveling-mode phenomenon, which is different from the stationary vibration modes for the non-rotating cylinders. After Bryan's work, Taranto and Lessen (1964) next investigated the influence of the Coriolis acceleration effect on the free vibration of a rotating thin-walled cylinder. Srinivasan and Lauterbach (1971) and Zohar and Aboudi (1973) presented the dynamic responses of rotating infinitely long and finite cylinders, respectively, and they focused on the shear deformation effect on the speeds of the traveling waves. Huang and Soedel (1988) developed a general model

*Corresponding author, Professor, E-mail: cpwu@mail.ncku.edu.tw

expansion technique for the forced vibration of such cylinders, and Huang and Hsu (1990) studied the resonant phenomena of a rotating cylinder subjected to a harmonic moving load. Chen *et al.* (1993) and Guo *et al.* (2001, 2002) developed a nine-node superparametric finite element for the vibration analysis of rotating cylinders, in which the effects of Coriolis acceleration, centrifugal force, initial tension and geometric non-linearity due to large deformation were considered. However, the rotating cylinders considered in these articles were all made of isotropic materials.

Fiber-reinforced composite materials, which consist of fiber and matrix materials that are bonded together, possess many advantageous material properties, and thus are gradually replacing isotropic materials in rotating shell structures, due to their high strength, stiffness and corrosion resistance, thermal and acoustical insulation, and low weight. Lam and Loy (1994, 1995a) presented the influence of rotation on the frequency characteristics of laminated composite and sandwich-type cylinders. Using the beam functions, Lam and Loy (1995b, 1998) then analyzed the effects of boundary conditions on the free vibration of the laminated composite cylinders, which was also studied by Lam and Loy (1995c), Lam and Wu (1999) and Kadivar and Samani (2000), using the assorted classical shell, first-order shear deformation and layer-wise lamination theories (CST, FSDT, LWLT), respectively. These studies are helpful to better understand the influence of rotation on the frequencies and vibration-mode characteristics of homogeneous isotropic and multilayered composite cylinders, with most based on the approximate two-dimensional (2D) CST, and a few on the FSDT and LWLT.

In recent decades, a new class of materials, known as functionally graded materials (FGMs), has been developed and is increasingly being used in various engineering applications. Unlike the conventional multilayered composite structures, the material properties of which suddenly change at the interface between adjacent layers, those of FGM plates and shells gradually and continuously vary through the thickness coordinate. It has been reported that some of the drawbacks that often occur in laminated composite plates and shells can be overcome with these materials, such as residual thermal stress concentration and delamination. The development of theoretical methodologies and numerical modeling for the analyses of FGM plates and shells is thus important for their reliable design and application.

Some 2D and 3D approaches for the dynamic analysis of non-rotating, rather than rotating, FGM cylindrical and conical shells, have been presented. Based on the CST and FSDT, Sepiani *et al.* (2010) studied the free vibration and buckling of a two-layered cylindrical shell made of inner FGM layer and outer isotropic one, which is subjected to static and periodic axial forces. On the basis of Love's shell theory combined with the von Karman-type of nonlinearity, Haddadpour *et al*. (2007) investigated the free vibration characteristics of FGM cylindrical shells, in which four sets of in-plane boundary conditions was considered, and the material properties were assumed to be temperature-dependant and gradually changed in the thickness coordinate. Applying the variable substitution technique, superposition method, and separation of variables, Wang *et al.* (2009) presented the exact solutions of torsional vibration of FGM finite hollow cylinders with various boundary conditions. Yas and Garmsiri (2010) presented the 3D solutions of free vibration problems of cylindrical shells with continuous grading reinforcement using the differential quadrature method. Wu and Tsai (2009) studied the cylindrical bending vibration of functionally graded (FG) piezoelectric shells using the method of multiple scales.

Some application of Reissner's mixed variational theorem (RMVT) to the analysis of laminated composite and FGM structures has been presented. The use of this theory to analyze laminated plate structures was examined by Carrera (2000a). In combination with different kinematic and kinetic models, the RMVT was also extensively used to a variety of analyses of multilayered shells by Carrera

(1999a,c). Carrera (2000b) undertook the assessment of mixed and classical theories on global and local response of multilayered orthotropic plates, in which more than forty theories were implemented and compared their results one another. Developments, ideas, and evaluations based upon RMVT in the modeling of multilayered plates and shells were summarized by Carrera (2001), in which Carrera concluded that the RMVT should be considered as a natural tool for multilayered structure analyses, just like the role of the principle of virtual displacements (PVD) playing in the analysis of isotropic single-layered structures.

Based on Carrera's unified formulation (CUF) (Carrera 2003), Carrera *et al.* (2010) and Cinefra *et al.* (2010) investigated the static and vibration problems of multilayered plates and shells embedding FGM layers, in which the order of each primary variable expanded in the thickness coordinate remained the same, and could be freely chosen, a variable kinematic model was used, as well as some PVD-based refined models and RMVT-based advanced models were obtained. A comprehensive literature review with regard to the 3D approaches for the analyses of multilayered composite and FG elastic and piezoelectric material plates and shells was undertaken by Wu *et al.* (2008), in which four major approaches, namely the Pagano, state space, power series expansion, and asymptotic methods, were drawn from the open literature, and derivations for the formulations of each approach and the comparisons of the results obtained using them were presented. Among these, the Pagano method is the most commonly and widely applied approach for multilayered composite plates and shells, but it can not be directly applied to the analysis of FGM plates/shells without further modifications.

In order to utilize the Pagano method for the analysis of FGM plates/shells, Wu *et al.* (2010) and Wu and Lu (2009) developed a modified Pagano method for the static and free vibration analyses of simply supported, FG magneto-electro-elastic plates, respectively, and this is further extended in the present analysis. The modifications to the original Pagano method are as follows: (a) The RMVT-based formulation, rather than PVD-based one is developed, in which the displacement and transverse stress components are adopted as the primary variables, so that both the lateral boundary conditions on the outer surfaces, in which the transverse stresses are prescribed, and the displacement and transverse stress continuity conditions at the interface between adjacent layers can be directly applied. (b) The sets of complex-valued solutions of system equations are transferred to the corresponding sets of real-valued solutions by means of Euler's formula for the purpose of computational efficiency. (c) A successive approximation (SA) method commonly used for the analysis of homogeneous isotropic and laminated composite cylindrical shells (Soldatos and Hadjigeorgiou 1990, Ye 2003), is adopted, and the FGM layers constituting the cylinders considered in this paper are artificially divided into a certain number of individual layers with an equal and small thickness, compared with the curvature radius. By the refinement manipulation, one may reasonably approximate the variable material coefficients and the radial coordinate of each layer to the constant material coefficients in an average thickness sense and the mid-surface radius of each layer, respectively, so that the system of thickness-varying differential equations for each individual layer can be reduced to a system of thickness-invariant differential equations. (d) A propagator matrix method is developed, so that the general solutions of system equations can be obtained layer-by-layer. These modifications make the Pagano method feasible for the 3D free vibration analysis of rotating and non-rotating multilayered FGM cylinders. It is noted that due to these changes, the computation in the implementation is independent of the total number of layers constituting the cylinder, and becomes less time-consuming than usual.

Due to the fact that the exact 3D free vibration analysis of rotating multilayered composite and FGM cylinders can not be found in the literature, and the modified Pagano method, based on the

RMVT, possesses many advantages, as noted above, we extensively applied it to this analysis, in which the material properties of each FGM layer of the cylinders are assumed to obey a power-law distribution of the volume fractions of the constituents, and the effects of Coriolis and centrifugal accelerations, as well as the initial hoop stress due to rotation, are considered in this RMVT-based formulation. A parameter study of the influence of the material-property gradient index, rotational speed, mid-surface radius-thickness ratio, and the thickness ratio of each layer on the natural frequencies of the rotating multilayered FGM circular hollow cylinders is undertaken. In addition, the free vibration of the non-rotating cylinders can be analyzed by simply letting the rotational speed be zero in this formulation, and the differences in the vibration characteristics between the rotating and non-rotating cylinders are also discussed.

2. Reissner's mixed variational theorem

A simply-supported, multilayered composite and FG elastic material circular hollow cylinder, rotating with a constant angular speed (Ω) with respect to the meridional direction, is considered, as shown in Fig. 1. A set of the cylindrical coordinates (x, θ, r) is located on the middle surface of the cylinder. The total thickness, length, mid-surface radius and thickness coordinate of the cylinder are h, L, R and ζ, respectively, and $r = R+\zeta$.

The linear constitutive equations valid for the nature of the symmetry class of elastic materials considered in this work are given by

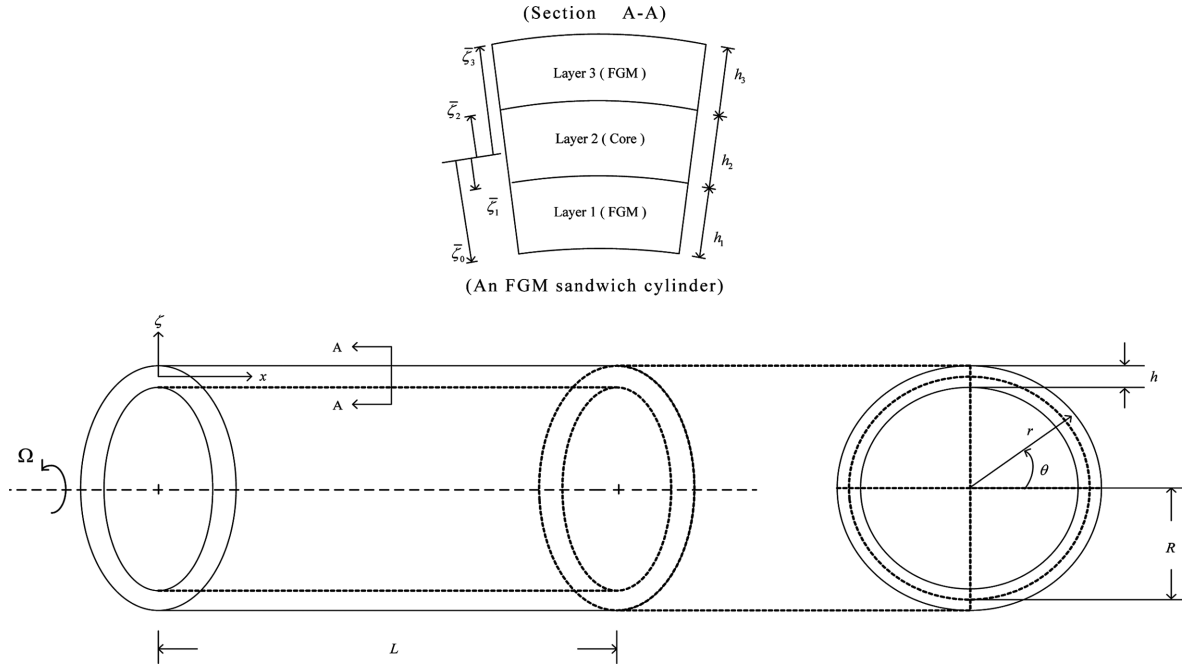

Fig. 1 The configuration and coordinates of a multilayered FGM circular hollow cylinder

$$\begin{Bmatrix}\sigma_x\\ \sigma_\theta\\ \sigma_r\\ \tau_{\theta r}\\ \tau_{xr}\\ \tau_{x\theta}\end{Bmatrix}=\begin{bmatrix}c_{11} & c_{12} & c_{13} & 0 & 0 & 0\\ c_{12} & c_{22} & c_{23} & 0 & 0 & 0\\ c_{13} & c_{23} & c_{33} & 0 & 0 & 0\\ 0 & 0 & 0 & c_{44} & 0 & 0\\ 0 & 0 & 0 & 0 & c_{55} & 0\\ 0 & 0 & 0 & 0 & 0 & c_{66}\end{bmatrix}\begin{Bmatrix}\varepsilon_x\\ \varepsilon_\theta\\ \varepsilon_r\\ \gamma_{\theta r}\\ \gamma_{xr}\\ \gamma_{x\theta}\end{Bmatrix} \tag{1}$$

where (σ_x, σ_θ, σ_r, $\tau_{\theta r}$, τ_{xr}, $\tau_{x\theta}$) and (ε_x, ε_θ, ε_r, $\gamma_{\theta r}$, γ_{xr}, $\gamma_{x\theta}$) are the stress and strain components, respectively, and c_{ij} (i, j=1-6) are the elastic coefficients, which are regarded as heterogeneous through the thickness (i.e., c_{ij} (ζ)).

The strain-displacement relationships are

$$\varepsilon_x = u_{x,x}+\frac{1}{2}[(u_{x,x})^2+(u_{\theta,x})^2+(u_{r,x})^2] \tag{2}$$

$$\varepsilon_\theta = r^{-1}u_{\theta,\theta}+r^{-1}u_r+\frac{1}{2}\left[\left(r^{-1}u_{\theta,\theta}+r^{-1}u_r\right)^2+\left(r^{-1}u_{r,\theta}-r^{-1}u_\theta\right)^2+\left(r^{-1}u_{x,\theta}\right)^2\right] \tag{3}$$

$$\varepsilon_r = u_{r,r}+\frac{1}{2}\left[\left(u_{x,r}\right)^2+\left(u_{\theta,r}\right)^2+\left(u_{r,r}\right)^2\right] \tag{4}$$

$$\gamma_{xr} = u_{x,r}+u_{r,x}+\left[\left(u_{x,x}\right)\left(u_{x,r}\right)+\left(u_{\theta,x}\right)\left(u_{\theta,r}\right)+\left(u_{r,x}\right)\left(u_{r,r}\right)\right] \tag{5}$$

$$\gamma_{\theta r} = u_{\theta,r}-r^{-1}u_\theta+r^{-1}u_{r,\theta}+\left[r^{-1}\left(u_{x,r}\right)\left(u_{x,\theta}\right)+r^{-1}\left(u_{\theta,r}\right)\left(u_{\theta,\theta}+u_r\right)+r^{-1}\left(u_{r,r}\right)\left(u_{r,\theta}-u_\theta\right)\right] \tag{6}$$

$$\gamma_{x\theta} = r^{-1}u_{x,\theta}+u_{\theta,x}+\left[r^{-1}\left(u_{x,x}\right)\left(u_{x,\theta}\right)+r^{-1}\left(u_{\theta,x}\right)\left(u_{\theta,\theta}+u_r\right)+r^{-1}\left(u_{r,x}\right)\left(u_{r,\theta}-u_\theta\right)\right] \tag{7}$$

in which u_i ($i = x, \theta, r$) are the displacement components, and the commas denote the partial differentiation of the suffix variables with respect to the spatial coordinates, which are x, θ and r.

It is noted that the nonlinear terms of the Lagrange strain ε_θ, which is given in Eq. (3), are considered for computing the force components due to the initial hoop stress, $\overline{\sigma}_\theta^0$, which is generated by the centrifugal effect due to rotation, and $\overline{\sigma}_\theta^0=\rho r^2\,\Omega^2$, in which ρ denotes the mass density. The initial stress is an important restoring mechanism, which approximately reduces a nonlinear problem to a linear one disturbed from equilibrium and subjected to the initial state of stresses, and it has also been commonly used in the linear buckling and vibration analyses of plates and shells, the details of which have been described by Leissa (1973, 1995), Sodel (1993), and Wu and Chiu (2001, 2002). In the subsequent derivation of the Euler-Lagrange equations of this rotating cylinder, the linear approximation approach will be adopted, and the strain energy due to this initial hoop stress is thus given as

$$U_i = \int_{-h/2}^{h/2}\int_0^{2\pi}\int_0^L \overline{\sigma}_\theta^0\,\varepsilon_\theta^{NL}\,r\,dx\,d\theta\,d\zeta \tag{8}$$

where ε_θ^{NL} denotes the nonlinear terms of ε_θ, and is given as

$$\varepsilon_\theta^{NL} = \frac{1}{2}\left[\left(r^{-1}u_{\theta,\theta}+r^{-1}u_r\right)^2+\left(r^{-1}u_{r,\theta}-r^{-1}u_\theta\right)^2+\left(r^{-1}u_{x,\theta}\right)^2\right] \tag{9}$$

The velocity vector ($\vec{V}$) at any point of this cylinder is given by

$$\vec{V} = \frac{d\vec{r}}{dt} + (\Omega \vec{e}_x) \mathrm{x} \vec{r} \tag{10}$$

where $\vec{r}$ is the position vector, and it is given as $\vec{r} = u_x \vec{e}_x + u_\theta \vec{e}_\theta + u_r \vec{e}_r$; $\vec{e}_x$, $\vec{e}_\theta$ and $\vec{e}_r$ denote the unit vector in the x, θ and r directions, respectively; t is the time variable; and x is defined as the outer product between two vectors.

Substituting the position vector, mentioned above, into Eq. (10), we can rewrite the velocity vector as follows

$$\vec{V} = \dot{u}_x \vec{e}_x + (\dot{u}_\theta - \Omega u_r)\vec{e}_\theta + (\dot{u}_r + \Omega u_\theta)\vec{e}_r \tag{11}$$

where $\dot{u}_x, \dot{u}_\theta, \dot{u}_r$ denote the linear velocity components in the x, θ and r directions, respectively.

The kinetic energy of the rotating cylinder is given by

$$T = \frac{1}{2}\int_{-h/2}^{h/2}\int_0^{2\pi}\int_0^L \rho\left(\vec{V} \bullet \vec{V}\right) r\, dx\, d\theta\, d\zeta \tag{12}$$

where the symbol "·" is defined as the inner product between two vectors.

Substituting Eq. (11) into Eq. (12), we can rewrite the kinetic energy of the rotating cylinder as follows

$$T = \frac{1}{2}\int_{-h/2}^{h/2}\int_0^{2\pi}\int_0^L \rho\left[\dot{u}_x^2 + \dot{u}_\theta^2 + \dot{u}_r^2 + 2\Omega(u_\theta \dot{u}_r - u_r \dot{u}_\theta) + \Omega^2\left(u_\theta^2 + u_r^2\right)\right] r\, dx\, d\theta\, d\zeta \tag{13}$$

in which the first three terms are due to the contribution of the linear velocity components in the x, θ and r directions, respectively, and the fourth and fifth terms are that of the Coriolis and centrifugal effects, respectively.

The Reissner energy functional, related to this 3D free vibration analysis of rotating multilayered FGM cylinders, is written in the form of

$$I_R = \int_{t_1}^{t_2} (T - V_R - U_i)dt \tag{14}$$

where T and U_i denote the kinetic energy and strain energy due to this initial hoop stress, respectively, and are given in Eqs. (13) and (8); and V_R stands for the RMVT-based potential energy, and is given as

$$\begin{aligned} V_R = {} & \int_{-h/2}^{h/2}\int_0^{2\pi}\int_0^L \left[\sigma_x \varepsilon_x + \sigma_\theta \varepsilon_\theta + \sigma_r \varepsilon_r + \tau_{xr}\gamma_{xr} + \tau_{\theta r}\gamma_{\theta r} + \tau_{x\theta}\gamma_{x\theta} - B(\sigma_{ij})\right] r\, dx\, d\theta\, d\zeta \\ & - \int_{-h/2}^{h/2}\int_{\Gamma_\sigma} \overline{T}_i u_i\, d\Gamma\, d\zeta - \int_{-h/2}^{h/2}\int_{\Gamma_u} T_i (u_i - \overline{u}_i)\, d\Gamma\, d\zeta \end{aligned} \tag{15}$$

where Γ_σ and Γ_u denote the portions of the edge boundary, in which the surface tractions $\overline{T}_i$ ($i = x$, θ and r) and surface displacements $\overline{u}_i$ ($i = x$, θ and r) are prescribed, respectively; and $B(\sigma_{ij})$ is the complementary energy density function.

In the present RMVT-based formulation, we take the elastic displacement and transverse stress components as the primary variables subject to variation, and the strain and in-plane stress components are the dependent variables, which can be expressed in terms of the primary variables, as follows:

$$\varepsilon_x = \partial B / \partial \sigma_x = u_{x,x} \tag{16}$$

$$\varepsilon_\theta = \partial B / \partial \sigma_\theta = r^{-1} u_{\theta,\theta} + r^{-1} u_r \tag{17}$$

$$\varepsilon_r = \partial B / \partial \sigma_r = -Q_{13} u_{x,x} - \left(Q_{23} r^{-1}\right) u_{\theta,\theta} - \left(Q_{23} r^{-1}\right) u_r + \left(c_{33}^{-1}\right) \sigma_r \tag{18}$$

$$\gamma_{xr} = \partial B / \partial \tau_{xr} = \left(c_{55}^{-1}\right) \tau_{xr} \tag{19}$$

$$\gamma_{\theta r} = \partial B / \partial \tau_{\theta r} = \left(c_{44}^{-1}\right) \tau_{\theta r} \tag{20}$$

$$\gamma_{x\theta} = \partial B / \partial \tau_{x\theta} = r^{-1} u_{x,\theta} + u_{\theta,x} \tag{21}$$

$$\boldsymbol{\sigma}_p = \mathbf{Q}_p \mathbf{B}_1 \mathbf{u} + \mathbf{Q}_p \mathbf{B}_2 u_r + \mathbf{Q}_r \sigma_r \tag{22}$$

where $\boldsymbol{\sigma}_p = \{\sigma_x \ \sigma_\theta \ \tau_{x\theta}\}^T$, $\mathbf{u} = \{u_x \ u_\theta\}^T$, $\mathbf{Q}_p = \begin{bmatrix} Q_{11} & Q_{12} & 0 \\ Q_{12} & Q_{22} & 0 \\ 0 & 0 & Q_{66} \end{bmatrix}$, $\mathbf{B}_1 = \begin{bmatrix} \partial_x & 0 \\ 0 & r^{-1}\partial_\theta \\ r^{-1}\partial_\theta & \partial_x \end{bmatrix}$

$\mathbf{B}_2 = \begin{bmatrix} 0 \\ r^{-1} \\ 0 \end{bmatrix}$, $\mathbf{Q}_r = \begin{bmatrix} Q_{13} \\ Q_{23} \\ 0 \end{bmatrix}$, $Q_{ij} = c_{ij} - \left(c_{i3}\, c_{j3} / c_{33}\right)$ (i, j=1, 2 and 6)

$Q_{i3} = c_{i3}/c_{33}$ ($i = 1$ and 2).

Substituting Eqs. (1), (8), (13) and (15)-(22) into Eq. (14) and imposing the stationary principle of the Reissner energy functional yields

$$\delta I_R = \int_{t_1}^{t_2} (\delta T - \delta V_R - \delta U_i) dt = 0 \tag{23}$$

where

$$\int_{t_1}^{t_2} \delta T \, dt = \int_{t_1}^{t_2} \int_{-h/2}^{h/2} \int_0^{2\pi} \int_0^L \left[\rho r\left(\dot{u}_x \, \delta \dot{u}_x + \dot{u}_\theta \, \delta \dot{u}_\theta + \dot{u}_r \, \delta \dot{u}_r\right) + \rho r \Omega^2 \left(u_\theta \, \delta u_\theta + u_r \, \delta u_r\right) \right.$$
$$\left. \rho r \Omega \left(u_\theta \, \delta \dot{u}_r + \dot{u}_r \, \delta u_\theta - \dot{u}_\theta \, \delta u_r - u_r \, \delta \dot{u}_\theta\right)\right] dx \, d\theta \, d\zeta \, dt$$

$$\int_{t_1}^{t_2} \delta V_R \, dt = \int_{t_1}^{t_2} \int_{-h/2}^{h/2} \int_0^{2\pi} \int_0^L \left\{ r \sigma_x \delta u_{x,x} + \sigma_\theta \left(\delta u_{\theta,\theta} + \delta u_r\right) + \tau_{x\theta} \left(\delta u_{x,\theta} + r \delta u_{\theta,x}\right) + r \sigma_r \, \delta u_{r,\zeta} \right.$$
$$+ \tau_{\theta r} \left(\delta u_{r,\theta} + r \delta u_{\theta,\zeta} - \delta u_\theta\right) + r \tau_{xr} \left(\delta u_{r,x} + \delta u_{x,\zeta}\right)$$
$$+ \left[r u_{r,\zeta} + r Q_{13} u_{x,x} + Q_{23} \left(u_{\theta,\theta} + u_r\right) - \left(r \sigma_r / c_{33}\right)\right] \delta \sigma_r$$
$$\left. + \left[\left(r u_{\theta,\zeta} - u_\theta + u_{r,\theta} - r \tau_{\theta r} / c_{44}\right)\right] \delta \tau_{\theta r} + \left(r u_{x,\zeta} + r u_{r,x} - r \tau_{xr} / c_{55}\right) \delta \tau_{xr} \right\} dx \, d\theta \, d\zeta \, dt$$
$$- \int_{t_1}^{t_2} \int_{-h/2}^{h/2} \int_{\Gamma_\sigma} \overline{T}_i \, \delta u_i \, d\Gamma \, d\zeta \, dt - \int_{t_1}^{t_2} \int_{-h/2}^{h/2} \int_{\Gamma_u} \delta T_i \left(u_i - \overline{u}_i\right) d\Gamma \, d\zeta \, dt$$

$$\int_{t_1}^{t_2} \delta U_i \, dt = \int_{t_1}^{t_2} \int_{-h/2}^{h/2} \int_0^{2\pi} \int_0^L \left[\overline{\sigma}_\theta^0 \left(r^{-1} u_{\theta,\theta} + r^{-1} u_r\right)\left(\delta u_{\theta,\theta} + \delta u_r\right) + \overline{\sigma}_\theta^0 \left(r^{-1} u_{r,\theta} - r^{-1} u_\theta\right)\left(\delta u_{r,\theta} - \delta u_\theta\right) \right.$$
$$\left. + \overline{\sigma}_\theta^0 \left(r^{-1} u_{x,\theta}\right) \delta u_{x,\theta} \right] dx \, d\theta \, d\zeta \, dt$$

After performing the integration by parts and using Green's theorem for the terms, related to the partial differentiation of the first variation of the assorted primary variables with respect to the spatial coordinates (x, θ and ζ) and time (t), in Eq. (23), we finally obtain the Euler-Lagrange equations of the 3D free vibration problem of rotating cylinders from the domain integral terms and the admissible boundary conditions from the boundary integral terms, which are written as follows:

The Euler-Lagrange equations are

$$\delta u_x: \ \tau_{xr,\zeta} = -\sigma_{x,x} - \left(r^{-1}\tau_{x\theta,\theta}\right) - \left(r^{-1}\tau_{xr}\right) - \overline{\sigma}_\theta^0 r^{-2}\left(u_{x,\theta\theta}\right) + \rho\left(u_{x,tt}\right) \tag{24}$$

$$\delta u_\theta: \ \tau_{\theta r,\zeta} = -\tau_{x\theta,x} - \left(r^{-1}\sigma_{\theta,\theta}\right) - 2\left(r^{-1}\tau_{\theta r}\right) - \overline{\sigma}_\theta^0 r^{-2}\left(2u_{r,\theta} + u_{\theta,\theta\theta} - u_\theta\right) + \rho\left(u_{\theta,tt} + 2\Omega u_{r,t} - \Omega^2 u_\theta\right) \tag{25}$$

$$\delta u_r: \ \sigma_{r,\zeta} = -\tau_{xr,x} - \left(r^{-1}\tau_{\theta r,\theta}\right) - \left(r^{-1}\sigma_r\right) + \left(r^{-1}\sigma_\theta\right) - \overline{\sigma}_\theta^0 r^{-2}\left(u_{r,\theta\theta} - 2u_{\theta,\theta} - u_r\right) + \rho\left(u_{r,tt} - 2\Omega u_{\theta,t} - \Omega^2 u_r\right) \tag{26}$$

$$\delta \tau_{xr}: \ u_{x,\zeta} = -u_{r,x} + \left(\tau_{xr}/c_{55}\right) \tag{27}$$

$$\delta \tau_{\theta r}: \ u_{\theta,\zeta} = \left(r^{-1}u_\theta\right) - \left(r^{-1}u_{r,\theta}\right) + \left(\tau_{\theta r}/c_{44}\right) \tag{28}$$

$$\delta \sigma_r: \ u_{r,\zeta} = -Q_{13}u_{x,x} - Q_{23}r^{-1}u_{\theta,\theta} - Q_{23}r^{-1}u_r + \left(\sigma_r/c_{33}\right) \tag{29}$$

The lateral boundary conditions are

$$\lfloor \tau_{xr} \ \ \tau_{\theta r} \ \ \sigma_r \rfloor = [0 \ \ 0 \ \ 0] \ \text{ on } \ \zeta = \pm h/2 \,. \tag{30}$$

The edge boundary conditions are

$$\sigma_x n_1 + \tau_{x\theta} n_2 = \overline{T}_x \ \text{ or } \ u_x = \overline{u}_x \tag{31a}$$

$$\tau_{x\theta} n_1 + \sigma_\theta n_2 = \overline{T}_\theta \ \text{ or } \ u_\theta = \overline{u}_\theta \tag{31b}$$

$$\tau_{xr} n_1 + \tau_{\theta r} n_2 = \overline{T}_r \ \text{ or } \ u_r = \overline{u}_r \tag{31c}$$

where n_1 and n_2 denote the direction cosines of the unit normal vector along the edge.

3. The state space equations

These Euler-Lagrange equations, given in Eqs. (24)-(29), can be rewritten in a matrix form, which is a set of state space equations in terms of the primary field variables, as follows

$$\frac{\partial \mathbf{F}(x,\theta,\zeta)}{\partial \zeta} = (\mathbf{K} + \mathbf{K}_1 + \mathbf{K}_2 + \mathbf{K}_3 + \mathbf{M})\mathbf{F}(x,\theta,\zeta) \tag{32}$$

where $\mathbf{F}(x,\theta,\zeta) = \{u_x \ \ u_\theta \ \ u_r \ \ \tau_{xr} \ \ \tau_{\theta r} \ \ \sigma_r\}^T$

$$\mathbf{K}=\begin{bmatrix} 0 & 0 & k_{13} & k_{14} & 0 & 0 \\ 0 & k_{22} & k_{23} & 0 & k_{25} & 0 \\ k_{31} & k_{32} & k_{33} & 0 & 0 & k_{36} \\ k_{41} & k_{42} & k_{43} & -k_{22} & 0 & k_{31} \\ k_{42} & k_{52} & k_{53} & 0 & k_{55} & k_{32} \\ -k_{43} & -k_{53} & k_{63} & k_{13} & k_{23} & k_{66} \end{bmatrix},\quad \mathbf{K}_1=\left(-\overline{\sigma}_\theta^0\right)\begin{bmatrix} 0 & 0 & 0 & 0 & 0 & 0 \\ 0 & 0 & 0 & 0 & 0 & 0 \\ 0 & 0 & 0 & 0 & 0 & 0 \\ k_{41}^{(1)} & 0 & 0 & 0 & 0 & 0 \\ 0 & k_{52}^{(1)} & k_{53}^{(1)} & 0 & 0 & 0 \\ 0 & -k_{53}^{(1)} & k_{52}^{(1)} & 0 & 0 & 0 \end{bmatrix}$$

$$\mathbf{K}_2=\begin{bmatrix} 0 & 0 & 0 & 0 & 0 & 0 \\ 0 & 0 & 0 & 0 & 0 & 0 \\ 0 & 0 & 0 & 0 & 0 & 0 \\ 0 & 0 & 0 & 0 & 0 & 0 \\ 0 & k_{52}^{(2)} & 0 & 0 & 0 & 0 \\ 0 & 0 & k_{52}^{(2)} & 0 & 0 & 0 \end{bmatrix},\quad \mathbf{K}_3=\begin{bmatrix} 0 & 0 & 0 & 0 & 0 & 0 \\ 0 & 0 & 0 & 0 & 0 & 0 \\ 0 & 0 & 0 & 0 & 0 & 0 \\ 0 & 0 & 0 & 0 & 0 & 0 \\ 0 & 0 & k_{53}^{(3)} & 0 & 0 & 0 \\ 0 & -k_{53}^{(3)} & 0 & 0 & 0 & 0 \end{bmatrix}$$

$$\mathbf{M}=\begin{bmatrix} 0 & 0 & 0 & 0 & 0 & 0 \\ 0 & 0 & 0 & 0 & 0 & 0 \\ 0 & 0 & 0 & 0 & 0 & 0 \\ m_{41} & 0 & 0 & 0 & 0 & 0 \\ 0 & m_{41} & 0 & 0 & 0 & 0 \\ 0 & 0 & m_{41} & 0 & 0 & 0 \end{bmatrix}$$

$$k_{13}=-\partial_x,\ k_{14}=1/c_{55},\ k_{22}=r^{-1},\ k_{23}=-r^{-1}\partial_\theta,\ k_{25}=1/c_{44},\ k_{31}=-Q_{13}\partial_x$$

$$k_{32}=-(Q_{23}\,r^{-1})\partial_\theta,\ k_{33}=-Q_{23}\,r^{-1},\ k_{36}=1/c_{33},\ k_{41}=-(Q_{11}\partial_{xx}+Q_{66}\,r^{-2}\partial_{\theta\theta})$$

$$k_{42}=-(Q_{12}+Q_{66})r^{-1}\partial_{x\theta},\ k_{43}=-Q_{12}\,r^{-1}\partial_x,\ k_{52}=-(Q_{66}\partial_{xx}+Q_{22}\,r^{-2}\partial_{\theta\theta}),\ k_{53}=-Q_{22}\,r^{-2}\partial_\theta$$

$$k_{55}=-2\,r^{-1},\ k_{63}=Q_{22}\,r^{-2},\ k_{66}=(Q_{23}-1)/r,\ k_{41}^{(1)}=r^{-2}\partial_{\theta\theta},\ k_{52}^{(1)}=-r^{-2}+(r^{-2}\partial_{\theta\theta})$$

$$k_{53}^{(1)}=(2\,r^{-2})\partial_\theta,\ k_{52}^{(2)}=-\rho\Omega^2,\ k_{53}^{(3)}=2\rho\Omega\partial_t,\ m_{41}=\rho\partial_{tt}$$

$$Q_{ij}=c_{ij}-(c_{i3}\,c_{j3}/c_{33})\ \ (i,j=1,2,6),Q_{i3}=c_{i3}/c_{33}\ \ (i=1\text{ and }2).$$

It is seen in Eq. (32) that the angular speed (Ω) appears in matrices $\mathbf{K}_i$ (i = 1,2 and 3), which are related to the contributions of the effects of initial hoop stress, centrifugal and Coriolis accelerations, respectively, and can be separately evaluated based on their influence on the vibration characteristics of rotating cylinders. Because the Coriolis accelerations effect involves in the odd powers of the frequency variables, pairs of eigenvalues (or natural frequencies), corresponding to the backward and forward traveling waves of the rotating cylinders due to $\Omega > 0$ and $\Omega < 0$, respectively, will be obtained.

In addition, this formulation can be reduced to that of non-rotating cylinders by simply letting the angular speed be zero, which is given as

$$\frac{\partial \mathbf{F}(x,\theta,\zeta)}{\partial \zeta} = (\mathbf{K}+\mathbf{M})\mathbf{F}(x,\theta,\zeta) \tag{33}$$

According to Eq. (33), in which $\Omega = 0$, we will find later in this analysis that the traveling vibration modes of a rotating cylinder will be reduced to the stationary vibration modes of a non-rotating cylinder.

4. The modified pagano method

The free vibration of simply-supported, multilayered composite and FGM circular hollow cylinders, rotating with an angular speed with respect to the meridional coordinate, is studied in this paper using the modified Pagano method (Wu *et al.* 2010, Wu and Lu 2009).

The lateral surface conditions of the cylinders are given as follows

$$\sigma_r = \tau_{xr} = \tau_{\theta r} = 0 \quad \text{on} \quad \zeta = \pm h/2 \tag{34}$$

The edge boundary conditions of the cylinders are considered as fully simple supports, such that the following quantities are satisfied:

$$\sigma_x = u_\theta = u_r = 0 \quad \text{at} \quad x = 0 \quad \text{and} \quad x = L \tag{35}$$

4.1 The double Fourier series expansion method

The double Fourier series expansion method is used to reduce the system of partial differential equations, given in Eq. (32), to a system of ordinary differential equations. By satisfying the edge boundary conditions, given in Eq. (35), we express the primary variables in the following form

$$\left(u_x,\ \tau_{xr}\right) = \sum_{\hat{m}=0}^{\infty}\sum_{\hat{n}=0}^{\infty} \left(u_{\hat{m}\hat{n}}(\zeta),\ \tau_{xz\hat{m}\hat{n}}(\zeta)\right) \cos\left(\tilde{m}x\right) \cos\left(\hat{n}\theta + \omega_{\hat{m}\hat{n}}t\right) \tag{36}$$

$$\left(u_\theta,\ \tau_{\theta r}\right) = \sum_{\hat{m}=0}^{\infty}\sum_{\hat{n}=0}^{\infty} \left(v_{\hat{m}\hat{n}}(\zeta),\ \tau_{\theta z\hat{m}\hat{n}}(\zeta)\right) \sin\left(\tilde{m}x\right) \sin\left(\hat{n}\theta + \omega_{\hat{m}\hat{n}}t\right) \tag{37}$$

$$\left(u_r,\ \sigma_r\right) = \sum_{\hat{m}=0}^{\infty}\sum_{\hat{n}=0}^{\infty} \left(w_{\hat{m}\hat{n}}(\zeta),\ \ \sigma_{z\hat{m}\hat{n}}(\zeta)\right) \sin\left(\tilde{m}x\right) \cos\left(\hat{n}\theta + \omega_{\hat{m}\hat{n}}t\right) \tag{38}$$

where $\tilde{m} = \hat{m}\pi/L$, $\hat{m}$ and $\hat{n}$ denote the meridional half- and circumferential full-wave numbers, which are positive integers and zero; and $\omega_{\hat{m}\hat{n}}$ represents a certain unknown natural frequency.

For brevity, the symbols of summation are omitted in the following derivation. Substituting the equations in (36)-(38) in Eq. (32), we have the following equations

$$\frac{d\overline{\mathbf{F}}(\zeta)}{d\zeta} = \overline{\mathbf{K}}\overline{\mathbf{F}}(\zeta) \tag{39}$$

where $\overline{\mathbf{F}} = \{u_{\hat{m}\hat{n}}\ \ v_{\hat{m}\hat{n}}\ \ w_{\hat{m}\hat{n}}\ \ \tau_{xz\hat{m}\hat{n}}\ \ \tau_{\theta z\hat{m}\hat{n}}\ \ \sigma_{z\hat{m}\hat{n}}\}^T$ and the detailed expressions of the constant coefficients

($\bar{k}_{ij}$) in $\overline{\mathbf{K}}$ are omitted for brevity.

4.2 Theory of the homogeneous linear system

Eq. (39) represents a system of six simultaneously linear ordinary differential equations in terms of six primary variables. For a certain fixed value of the thickness coordinate, the coefficients of the system equations of Eq. (39) are constants. The general solution of Eq. (39) is

$$\overline{\mathbf{F}} = \mathbf{A}\ \mathbf{L} \tag{40}$$

where $\mathbf{L}$ is a 6x1 matrix of arbitrary constants; $\mathbf{A}$ is a fundamental matrix of Eq. (39) that is formed by six linearly independent solutions in the form of $\mathbf{A} = [\mathbf{A}_1\ \ \mathbf{A}_2\ \ \mathbf{A}_3\ \ \mathbf{A}_4\ \ \mathbf{A}_5\ \ \mathbf{A}_6]$, $\mathbf{A}_i = \mathbf{\Lambda}_i\, e^{\lambda_i \zeta}$ (i=1-6); λ_i and $\mathbf{\Lambda}_i$ are the eigenvalues and their corresponding eigenvectors of the coefficient matrix $\overline{\mathbf{K}}$ in Eq. (39).

If the coefficient matrix $\overline{\mathbf{K}}$ has a complex eigenvalue λ_1 (i.e., $\lambda_1 = \mathrm{Re}(\lambda_1) + i\mathrm{Im}(\lambda_1)$), then its complex conjugate λ_2 (i.e., $\lambda_2 = \mathrm{Re}(\lambda_1) - i\mathrm{Im}(\lambda_1)$) is also an eigenvalue because all of the coefficients of $\overline{\mathbf{K}}$ are real. In addition, $\mathbf{\Lambda}_{1,2} = \mathrm{Re}(\mathbf{\Lambda}_1) \pm i\mathrm{Im}(\mathbf{\Lambda}_1)$ are the corresponding eigenvectors of the complex conjugate pair $\lambda_{1,2}$. There is nothing wrong with these two complex-valued solutions in Eq. (39). However, we prefer to replace them with two linearly independent solutions involving only real-valued quantities according to Euler's formula in order to yield more efficient computational performance, and the resulting solutions are given by

$$\mathbf{A}_1 = e^{\mathrm{Re}(\lambda_1)\,\zeta}\left[\mathrm{Re}\left(\mathbf{\Lambda}_1\right)\cos\left(\mathrm{Im}\left(\lambda_1\right)\zeta\right) - \mathrm{Im}\left(\mathbf{\Lambda}_1\right)\sin\left(\mathrm{Im}\left(\lambda_1\right)\zeta\right)\right] \tag{41}$$

$$\mathbf{A}_2 = e^{\mathrm{Re}(\lambda_1)\,\zeta}\left[\mathrm{Re}\left(\mathbf{\Lambda}_1\right)\sin\left(\mathrm{Im}\left(\lambda_1\right)\zeta\right) + \mathrm{Im}\left(\mathbf{\Lambda}_1\right)\cos\left(\mathrm{Im}\left(\lambda_1\right)\zeta\right)\right] \tag{42}$$

On the basis of the previous set of linearly independent real-valued solutions, a propagator matrix method can then be developed for the analysis of multilayered composite hollow cylinders, and it can also be extended to the analysis of multilayered FGM hollow cylinders using an SA method (Soldatos and Hadjigeorgiou 1990, Ye 2003) where each FGM layer of the hollow cylinders is artificially divided into a finite number (N_L) of individual layers with an equal and small thickness for each individual layer in comparison with the mid-surface radius, and constant material properties, which are determined in an average thickness sense. The exact 3D solutions of multilayered FGM cylinders can then be gradually approached by increasing the number of N_L.

4.3 The propagator matrix method

In this paper, the modified Pagano method (Wu *et al.* 2010, Wu and Lu 2009) is extensively applied to the exact 3D free vibration analysis of rotating and non-rotating multilayered composite and FGM hollow cylinders, the through-thickness distributions of material properties of which are modified as the layerwise Heaviside functions and given by

$$c_{ij}(\zeta) = \sum_{m=1}^{N} c_{ij}^{(m)}[H(\zeta-\zeta_{m-1}) - H(\zeta-\zeta_m)] \tag{43}$$

where N denotes the total number of individual layers, constituting the cylinders, $H(\zeta)$ is the Heaviside function, ζ_{m-1} and ζ_m are the distances measured from the middle surface of the hollow cylinder to the bottom and top surfaces of the m^{th}-layer, respectively.

The general solution of the m^{th}-layer can be written as

$$\overline{\mathbf{F}}^{(m)}(\zeta) = \mathbf{A}^{(m)}(\zeta)\mathbf{L}^{(m)} \tag{44}$$

As $\zeta = \zeta_{m-1}$, according to Eq. (44) we obtain

$$\mathbf{L}^{(m)} = [\mathbf{A}^{(m)}(\zeta_{m-1})]^{-1}\overline{\mathbf{F}}_{m-1} \tag{45}$$

where $\overline{\mathbf{F}}_{m-1}$ denotes the vector of primary field variables at the interface between the (m-1$^{\text{th}}$) and m^{th}-layers and $\overline{\mathbf{F}}_{m-1} = \overline{\mathbf{F}}^{(m)}(\zeta = \zeta_{m-1})$.

As $\zeta = \zeta_m$, using Eqs. (44) and (45), we obtain

$$\overline{\mathbf{F}}_m = \mathbf{R}_m\overline{\mathbf{F}}_{m-1} \tag{46}$$

where $\mathbf{R}_m = \mathbf{A}^{(m)}(\zeta_m)[\mathbf{A}^{(m)}(\zeta_{m-1})]^{-1}$.

By analogy, the vectors of primary field variables between the top and bottom surfaces of the cylinder (i.e., $\overline{\mathbf{F}}_N$ and $\overline{\mathbf{F}}_0$) are linked by

$$\overline{\mathbf{F}}_N = \mathbf{R}_N\,\overline{\mathbf{F}}_{(N-1)} = \mathbf{R}_N\,\mathbf{R}_{(N-1)}\cdots\mathbf{R}_1\,\overline{\mathbf{F}}_0 \tag{47}$$

By defining a symbol of consecutive multiplication, we rewrite Eq. (47) in the form of

$$\overline{\mathbf{F}}_N = \left(\prod_{m=1}^{N}\mathbf{R}_m\right)\overline{\mathbf{F}}_0\,, \tag{48}$$

where $\prod_{m=1}^{N}\mathbf{R}_m$ is a 6x6 matrix and given as $\prod_{m=1}^{N}\mathbf{R}_m = \mathbf{R}_N\,\mathbf{R}_{(N-1)}\cdots\mathbf{R}_2\,\mathbf{R}_1$.

Eq. (48) represents a set of six simultaneous algebraic equations. Imposing the boundary conditions prescribed on the lateral surfaces, we may rewrite it as

$$\begin{bmatrix}\overline{\mathbf{F}}_u\\ \mathbf{0}\end{bmatrix} = \begin{bmatrix}\mathbf{R}_{\mathrm{II}} & \mathbf{R}_{\mathrm{I\,II}}\\ \mathbf{R}_{\mathrm{II\,I}} & \mathbf{R}_{\mathrm{II\,II}}\end{bmatrix}\begin{bmatrix}\overline{\mathbf{F}}_b\\ \mathbf{0}\end{bmatrix} \tag{49}$$

where $\overline{\mathbf{F}}_u$ and $\overline{\mathbf{F}}_b$ denote the unknown variables on the upper and bottom surfaces, respectively, and $\overline{\mathbf{F}}_u = \{\, u_{\hat{m}\hat{n}}^{(N)}(\zeta = 0.5h) \quad v_{\hat{m}\hat{n}}^{(N)}(\zeta = 0.5h) \quad w_{\hat{m}\hat{n}}^{(N)}(\zeta = 0.5h)\,\}^T$ and $\overline{\mathbf{F}}_b = \{u_{\hat{m}\hat{n}}^{(1)}(\zeta = -0.5h) \quad v_{\hat{m}\hat{n}}^{(1)}(\zeta = -0.5h)$ $w_{\hat{m}\hat{n}}^{(1)}(\zeta = -0.5h)\,\}^T$.

According to Eq. (49), we have a set of homogeneous equations as

$$\mathbf{R}_{\mathrm{II\,I}}\,\overline{\mathbf{F}}_b = \mathbf{0} \tag{50}$$

where $\mathbf{R}_{\mathrm{II\,I}}$ is a 3x3 matrix, the coefficients of which are related to the given angular velocity (Ω) and the circular frequency ($\omega_{\hat{m}\hat{n}}$) to be determined.

A nontrivial solution of Eq. (50) exists if the determinant of the coefficient matrix vanishes. Hence, the natural frequencies of the rotating hollow cylinder with a given angular speed (Ω) and set of fixed values ($\hat{m}$, $\hat{n}$) can be obtained by

$$R(\omega_{\hat{m}\hat{n}}) = |\mathbf{R}_{\mathbf{II}\,\mathbf{I}}| = 0 \tag{51}$$

Eq. (51) is the so-called charateristic equation. Because the determinant of $\mathbf{R}_{\mathbf{II}\,\mathbf{I}}$, $R(\omega_{\hat{m}\hat{n}})$, yields an implicit, rather than explicit, function of $\omega_{\hat{m}\hat{n}}$, a bisection method is used to determine the roots of Eq. (51).

Once Eq. (51) is solved, the eigenvalues and their corresponding eigen vectors (i.e., the modal values of $\overline{\mathbf{F}}_b$ and $\overline{\mathbf{F}}_u$, can be determined from Eqs. (50) and (49), respectively. Afterwards, the modal values of the primary variables through the thickness coordinate of the cylinder can be obtained by

$$\overline{\mathbf{F}}^{(m)}(\zeta) = \mathbf{A}^{(m)}(\zeta)[\mathbf{A}^{(m)}(\zeta_{m-1})]^{-1}\overline{\mathbf{F}}_{m-1} = \mathbf{A}^{(m)}(\zeta)[\mathbf{A}^{(m)}(\zeta_{m-1})]^{-1}\left(\prod_{i=1}^{m-1}\mathbf{R}_i\right)\overline{\mathbf{F}}_0 \tag{52}$$

The corresponding set of dependent variables can then be obtained using Eq. (22).

5. Illustrative examples

5.1 Rotating single-layer isotropic cylinders

The free vibration analysis of infinitely long rotating single-layer isotropic hollow cylinders is studied in Table 1 using this modified Pagano method, in which $\hat{m} = 0$ and $\hat{n} = 2\text{-}10$; $\Omega = 0$, 0.1π and 0.2π (rad/sec); $R/h = 500$ and $R = 1$ m. Because the radial coordinate (r) in the system equations of this homogeneous cylinder is still variant, the SA method is applied to yield the convergent solutions, in which N_L is taken to be 20. The Poisson's ratio (υ), Young's modulus (E) and mass density (ρ) in this example are taken as $\upsilon = 0.3$, E = 4.8265 GPa and $\rho = 1314$ Kg/m^3; and the dimensionless natural frequency parameter ($\overline{\omega}$) is defined as $\overline{\omega} = \omega R\sqrt{(1-\upsilon^2)\rho/E}$.

As mentioned above, pairs of natural frequency parameters, corresponding to the backward and forward traveling waves of the rotating cylinders (i.e., $\overline{\omega}_b$ and $\overline{\omega}_f$) due to the positive and negative rotational speeds (i.e., $\Omega > 0$ and $\Omega < 0$), respectively, are obtained. In Table 1, the present solutions of rotating thin cylinders are also compared with those obtained from a simplified formula given by Chen *et al*. (1993) and the generalized differential quadrature (GDQ) method by Hua and Lam (2001). It is shown that the present solutions of the least natural frequency parameters corresponding to backward and forward traveling waves for different vibration modes are in excellent agreement with those solutions obtained from the GDQ method by Hua and Lam (2001). Moreover, when $\Omega = 0$, the present solutions of the least natural frequency parameters corresponding to backward and forward traveling waves merge to an identical one corresponding to the stationary vibration modes of a non-rotating cylinder, and again these results are in excellent agreement with the available solutions in the literature (Chen *et al.* 1993).

5.2 Rotating FGM sandwich cylinders

In this case, the free vibration of simply supported, rotating FGM sandwich cylinders, which consist of FGM face-sheets and a homogeneous core, is studied using a modified Pagano method. The volume fraction of each layer constituting the cylinder is given as

Table 1 The least natural frequency parameters of the infinitely long rotating single-layer isotropic hollow cylinder for different vibration modes and rotational speeds, in which $R/h = 500$

Ω (rad/s)	$\hat{n}$	Present		Chen [9]		Hua and Lam [43]	
		$\overline{\omega}_b$	$\overline{\omega}_f$	$\overline{\omega}_b$	$\overline{\omega}_f$	$\overline{\omega}_b$	$\overline{\omega}_f$
0.0	2	0.0015492	0.0015492	0.0015492	0.0015492	NA	NA
	3	0.0043818	0.0043818	0.0043818	0.0043818	NA	NA
	4	0.0084016	0.0084016	0.0084017	0.0084017	NA	NA
	5	0.0135871	0.0135871	0.0135873	0.0135873	NA	NA
	6	0.0199318	0.0199318	0.0199323	0.0199323	NA	NA
	7	0.0274334	0.0274334	0.0274343	0.0274343	NA	NA
	8	0.0360906	0.0360906	0.0360922	0.0360922	NA	NA
	9	0.0459029	0.0459029	0.0459055	0.0459055	NA	NA
	10	0.0568700	0.0568700	0.0568740	0.0568740	NA	NA
0.1π	2	0.0016856	0.0014354	0.0016802	0.0014301	0.0016903	0.0014401
	3	0.0044916	0.0043040	0.0044779	0.0042903	0.0044760	0.0043062
	4	0.0084933	0.0083461	0.0084766	0.0083294	0.0084554	0.0083082
	5	0.0136664	0.0135461	0.0136483	0.0135280	0.0136516	0.0135313
	6	0.0200023	0.0199009	0.0199836	0.0198822	0.0199958	0.0198944
	7	0.0274973	0.0274097	0.0274785	0.0273909	0.0274945	0.0274069
	8	0.0361494	0.0360725	0.0361310	0.0360540	0.0361489	0.0360720
	9	0.0459578	0.0458891	0.0459401	0.0458715	0.0459592	0.0458905
	10	0.0569217	0.0568597	0.0569052	0.0568433	0.0569249	0.0568629
0.2π	2	0.0018442	0.0013438	0.0018232	0.0013228	0.0018625	0.0013621
	3	0.0046332	0.0042579	0.0045788	0.0042035	0.0045144	0.0041391
	4	0.0086210	0.0083266	0.0085541	0.0082597	0.0085872	0.0082928
	5	0.0137838	0.0135433	0.0137109	0.0134704	0.0137716	0.0135310
	6	0.0201121	0.0199093	0.0200361	0.0198332	0.0201074	0.0199045
	7	0.0276013	0.0274262	0.0275236	0.0273484	0.0275998	0.0274247
	8	0.0362489	0.0360950	0.0361705	0.0360165	0.0362495	0.0360955
	9	0.0460536	0.0459163	0.0459752	0.0458379	0.0460558	0.0459185
	10	0.0570145	0.0568907	0.0569368	0.0568129	0.0570184	0.0568945

$$\Gamma^{(1)}(\zeta) = \left(\frac{\zeta - \overline{\zeta}_0}{\overline{\zeta}_1 - \overline{\zeta}_0}\right)^{\kappa_p} \text{ when } \overline{\zeta}_0 \le \zeta \le \overline{\zeta}_1 \tag{53a}$$

$$\Gamma^{(2)}(\zeta) = 1 \text{ when } \overline{\zeta}_1 \le \zeta \le \overline{\zeta}_2 \tag{53b}$$

$$\Gamma^{(3)}(\zeta) = \left(\frac{\zeta - \overline{\zeta}_3}{\overline{\zeta}_2 - \overline{\zeta}_3}\right)^{\kappa_p} \text{ when } \overline{\zeta}_2 \le \zeta \le \overline{\zeta}_3 \tag{53c}$$

in which the layer number is counted from the bottom layer of the cylinder; $\overline{\zeta}_0 = -\overline{\zeta}_3 = -h/2$ and $\overline{\zeta}_1 = -\overline{\zeta}_2 = -h_2/2$; κ_p denotes the material-property gradient index; when $\kappa_p = 0$, the FGM sandwich cylinder reduces to a single-layer homogeneous one, in which the material properties are E_t, υ_t and ρ_t, and when $\kappa_p = \infty$, the cylinder reduces to a homogeneous material three-layered one, in which the material properties of the face-sheets and core are (E_b, υ_b, ρ_b) and (E_t, υ_t, ρ_t), respectively.

Using the rule of mixture (Hill 1965), the effective engineering constants and mass density of each layer are written as follows

$$E^{(i)}(\zeta) = E_b + (E_t - E_b)\Gamma^{(i)}(\zeta) \quad (i = 1, 2 \text{ and } 3) \tag{54a}$$

$$\upsilon^{(i)} = \text{constant} \quad (i = 1, 2 \text{ and } 3) \tag{54b}$$

$$\rho^{(i)}(\zeta) = \rho_b + (\rho_t - \rho_b)\Gamma^{(i)}(\zeta) \quad (i = 1, 2 \text{ and } 3) \tag{54c}$$

where E_t and E_b denote the Young's modulus of the top and bottom surfaces of layer 1, which is the bottom layer, and ρ_t and ρ_b are their mass densities.

The dimensionless natural frequency parameter is defined as $\overline{\omega} = \omega(10R)\sqrt{\rho_b/E_b}$, and the top and bottom surfaces of layer 1 (the bottom layer) are considered to be aluminum (t) and alumina (b), respectively, the engineering constants and mass density of which are

$$\begin{aligned} E_t &= 70 \text{ GPa}, \ \upsilon_t = 0.3, \ \rho_t = 2707 \text{ kg/m}^3 \\ E_b &= 380 \text{ GPa}, \ \upsilon_b = 0.3, \ \rho_b = 3800 \text{ kg/m}^3 \end{aligned} \tag{55}$$

According to the SA method, we further divide each of the face-sheets and core layers constituting the cylinder into N_L layers with equal thickness and homogeneous material properties, which are determined in an average thickness sense and given as

$$\overline{g}^{(m)} = \frac{1}{\Delta\zeta_m}\int_{\zeta_{m-1}}^{\zeta_m} [g_b + (g_t - g_b)\Gamma^{(m)}(\zeta)]d\zeta \qquad (m = 1\text{–}N_L), \tag{56}$$

in which g represents E and ρ, $\rho\zeta_m = \Delta\zeta_m = \zeta_m - \zeta_{m-1}$, and ζ_m and ζ_{m-1} denote the distances measured from the middle-surface of the cylinder to the top and bottom surfaces of the m^{th}-divided-layer.

Table 2 shows the convergence studies with regard to the present solutions of least natural frequency parameters of rotating FGM sandwich cylinders for different vibration modes with a rotational speed $\Omega = 10\pi$ (rad/s), in which the geometric parameters are $L/R = 5$, $R/h = 10$, $R = 1$ m, $h_1{:}h_2{:}h_3 = h/3{:}h/3{:}h/3$, the material-property gradient index $\kappa_p = 3$, and vibration mode numbers are $\hat{m} = 1\text{-}4$ and $\hat{n} = 0\text{-}5$. It is seen in Table 2 that the convergent solutions are obtained when the number of artificially divided layers (N_L) for each individual FGM or core layer is taken to be 20, and the relative errors of these solutions with $N_L = 20$ are below 0.05% when they are compared with those solutions obtained using $N_L = 40$. $N_L = 20$ is thus used in the subsequent examples if not mentioned otherwise. It is also seen in Table 2 that pairs of natural frequency parameters, corresponding to the backward and forward traveling waves of the rotating cylinders due to the positive and negative rotational speeds (i.e., $\Omega > 0$ and $\Omega < 0$), respectively, are obtained when $\hat{m} = 1\text{-}4$ and $\hat{n} = 1\text{-}5$, while these approach an identical value when $\hat{n} = 0$, which represents the axi-symmetrical vibration modes. The fundamental natural frequency parameter in this studied case occurs in the vibration mode of $(\hat{m}, \ \hat{n}) = (1, 2)$.

Figure 2 shows the effect of the rotational speed (Ω) on the frequency ratio (ω/ω_0) of the rotating FGM sandwich cylinders, in which $R/h = 50$ and 500, $L/R = 20$, $R = 1$ m, $h_1{:}h_2{:}h_3 = h/3{:}h/3{:}h/3$, $\kappa_p = 3$, $(\hat{m}, \ \hat{n}) = (1, 2)$, and ω and ω_0 denotes the least natural frequency of the rotating and non-rotating cylinders, respectively, and ω represents ω_b and ω_f due to $\Omega > 0$ and $\Omega < 0$, respectively. The influence of Coriolis and centrifugal effects on the natural frequencies of the FGM sandwich cylinder rotating with a fixed rotational speed is also examined in Fig. 2. It is seen in Fig. 2 that when both the Coriolis and centrifugal effects are considered, the least natural frequencies associated with

Table 2 Convergence studies of the present solutions of least natural frequency parameters of rotating FGM sandwich cylinders for different vibration modes ($\Omega = 10\pi$ rad/s)

$(\hat{m}, \hat{n})$	$N_L = 2$		$N_L = 4$		$N_L = 8$		$N_L = 12$		$N_L = 20$		$N_L = 40$	
	$\overline{\omega}_b$	$\overline{\omega}_f$	$\overline{\omega}_b$	$\overline{\omega}_f$	$\overline{\omega}_b$	$\overline{\omega}_f$	$\overline{\omega}_b$	$\overline{\omega}_f$	$\overline{\omega}_b$	$\overline{\omega}_f$	$\overline{\omega}_b$	$\overline{\omega}_f$
(1, 0)	3.241671	3.241671	3.241757	3.241757	3.241777	3.241777	3.241780	3.241780	3.241782	3.241782	3.241783	3.241783
(1, 1)	1.658404	1.598687	1.658498	1.598781	1.658521	1.598804	1.658525	1.598808	1.658527	1.598810	1.658528	1.598811
(1, 2)	1.120393	1.070352	1.127006	1.076967	1.128485	1.078448	1.128735	1.078698	1.128856	1.078819	1.128905	1.078867
(1, 3)	2.339639	2.302008	2.359874	2.322249	2.363998	2.326375	2.364616	2.326993	2.364887	2.327264	2.364986	2.327362
(1, 4)	4.230022	4.200673	4.263708	4.234368	4.269588	4.240250	4.270252	4.240913	4.270459	4.241120	4.270500	4.241162
(1, 5)	6.547496	6.523668	6.593115	6.569297	6.599187	6.575371	6.599387	6.575571	6.599199	6.575383	6.599020	6.575203
(2, 0)	6.482824	6.482824	6.482963	6.482963	6.482991	6.482991	6.482995	6.482995	6.482997	6.482997	6.482998	6.482998
(2, 1)	4.054339	3.993509	4.054825	3.993995	4.054940	3.994110	4.054960	3.994130	4.054971	3.994141	4.054975	3.994145
(2, 2)	2.417070	2.367773	2.422296	2.373001	2.423446	2.374151	2.423636	2.374341	2.423726	2.374431	2.423762	2.374467
(2, 3)	2.851962	2.814140	2.872367	2.834548	2.876430	2.838612	2.877016	2.839198	2.877265	2.839447	2.877352	2.839535
(2, 4)	4.562473	4.532774	4.597219	4.567526	4.603101	4.573409	4.603718	4.574025	4.603885	4.574193	4.603906	4.574213
(2, 5)	6.833498	6.809355	6.879948	6.855814	6.885855	6.861721	6.885957	6.861823	6.885696	6.861563	6.885479	6.861345
(3, 0)	8.225944	8.225944	8.226913	8.226913	8.227136	8.227136	8.227175	8.227175	8.227194	8.227194	8.227202	8.227202
(3, 1)	5.893595	5.838824	5.895213	5.840439	5.895581	5.840806	5.895644	5.840869	5.895675	5.840900	5.895688	5.840913
(3, 2)	3.979709	3.933205	3.986392	3.939886	3.987815	3.941309	3.988041	3.941534	3.988145	3.941638	3.988184	3.941678
(3, 3)	3.824648	3.787478	3.845674	3.808503	3.849695	3.812524	3.850237	3.813066	3.850452	3.813281	3.850521	3.813350
(3, 4)	5.194818	5.165020	5.230960	5.201164	5.236758	5.206962	5.237280	5.207484	5.237375	5.207580	5.237356	5.207560
(3, 5)	7.342010	7.317580	7.389635	7.365210	7.395211	7.370786	7.395138	7.370712	7.394752	7.370326	7.394469	7.370044
(4, 0)	8.412017	8.412017	8.415106	8.415106	8.415788	8.415788	8.415902	8.415902	8.415956	8.415956	8.415978	8.415978
(4, 1)	7.072336	7.031085	7.076586	7.035326	7.077506	7.036244	7.077654	7.036392	7.077724	7.036462	7.077751	7.036489
(4, 2)	5.418473	5.377070	5.428575	5.387165	5.430618	5.389207	5.430919	5.389508	5.431050	5.389638	5.431097	5.389685
(4, 3)	5.049001	5.013640	5.072367	5.037001	5.076569	5.041202	5.077074	5.041706	5.077246	5.041879	5.077290	5.041922
(4, 4)	6.112144	6.082793	6.150175	6.120821	6.155793	6.126439	6.156164	6.126810	6.156144	6.126790	6.156064	6.126709
(4, 5)	8.083075	8.058581	8.132083	8.107590	8.137108	8.112614	8.136769	8.112276	8.136195	8.111702	8.135816	8.111322

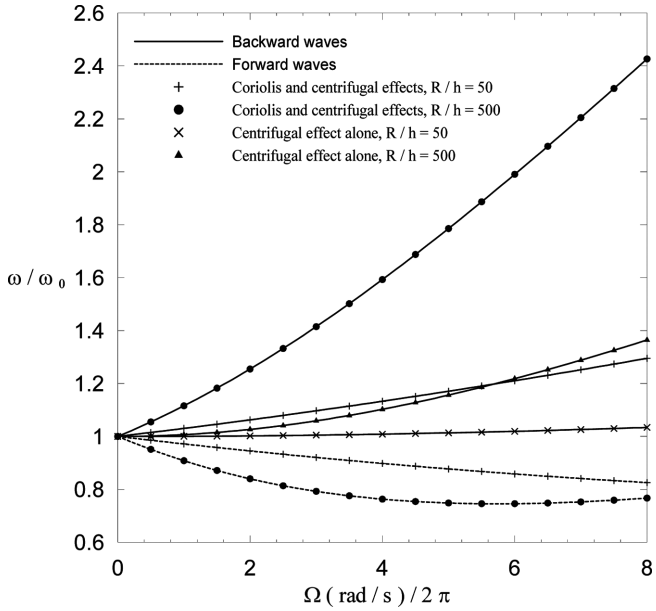

Fig. 2 Variations of the natural frequency ratio of a rotating FGM sandwich cylinder with the rotational speed for two different radius-to-thickness ratios

the backward traveling waves monotonically increase with the increase of the rotational speed, while those associated with the forward traveling waves first decrease with the increase of the rotational speed, and then gradually increase again. The deviation between the least natural frequencies corresponding to the backward and forward traveling waves increases when the rotational speed becomes faster. In addition, when only the centrifigual effect is considered, the coefficients of the $\mathbf{K}_i$ (i = 1-3) given in Eq. (32) are involved in even powers of the frequency variable, and thus the natural frequencies of backward and forward wave modes merge into identical values, which are slightly higher than the natural frequencies of a non-rotating cylinder. It is noted that the Coriolis effect is much more significant than the centrifugal one on the natural frequency parameters of a rotating cylinder, and the rotation effect on the natural frequencies of a rotating thin cylinder is much more significant than on those of a thick one.

Fig. 3 shows the effect of the rotational speed (Ω) on the natural frequency ratio (ω/ω_0) of the rotating FGM sandwich cylinders for different vibration modes, in which R/h = 500, L/R = 20, R = 1 m, h_1:h_2:h_3 = h/3:h/3:h/3, κ_p = 3, and ($\hat{m}$, $\hat{n}$) = (1, 2), (1, 4) and (2, 4). It is shown that the variations of the least natural frequencies with the rotational speed for the vibration modes of ($\hat{m}$, $\hat{n}$) = (1, 4) and (2, 4) are different from those for the above-mentioned vibration mode, ($\hat{m}$, $\hat{n}$) = (1, 2), in which the least natural frequencies of the non-rotating FGM sandwich cylinder are between those corresponding to the backward and forward traveling waves of the rotating one for the vibration mode ($\hat{m}$, $\hat{n}$) = (1, 2), while the least natural frequencies of the non-rotating FGM sandwich cylinder are below those corresponding to the backward and forward traveling waves of the rotating one for the vibration modes ($\hat{m}$, $\hat{n}$) = (1, 4) and (2, 4); and the least natural frequencies associated with the both backward and forward traveling waves always monotonically increase with the increase of the rotational speed for the vibration modes ($\hat{m}$, $\hat{n}$) = (1, 4) and (2, 4).

Fig. 4 shows the variations of the natural frequency ratios (ω/ω_0) of the rotating FGM sandwich

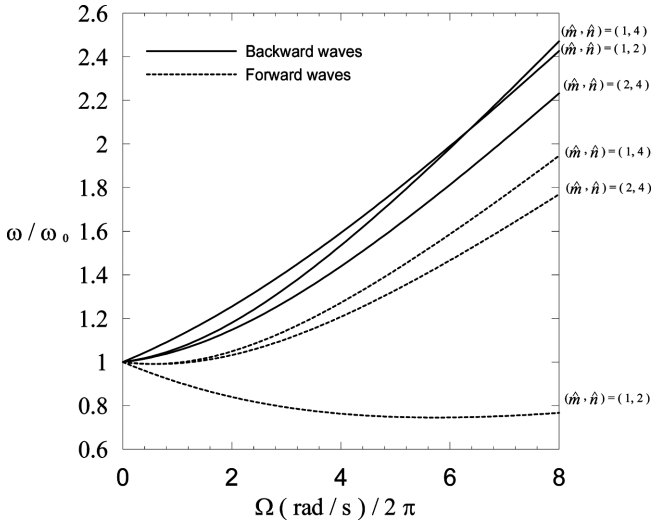

Fig. 3 Variations of the natural frequency ratio of a rotating FGM sandwich cylinder with the rotational speed for three different vibration modes

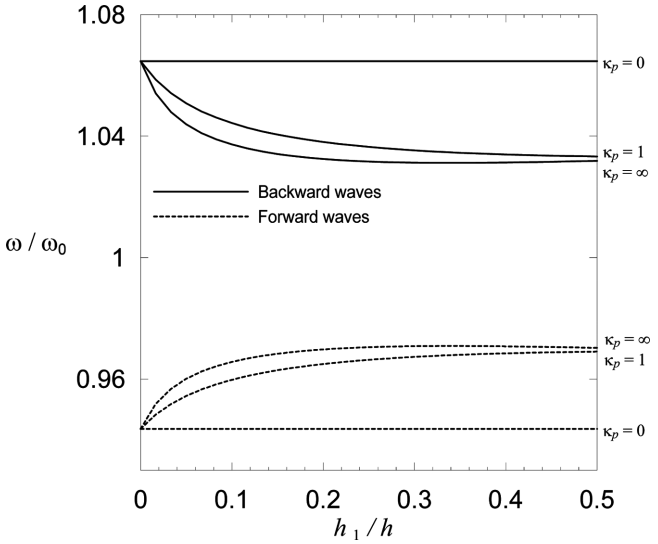

Fig. 4 Variations of the natural frequency ratio of a rotating FGM sandwich cylinder with the thickness ratio of h_1/h

cylinders with the thickness ratio (h_1/h) for different material-property gradient indexes, in which L/R=20, R/h=10, R=1 m, $(\hat{m}, \hat{n}) = (1, 2)$, $\Omega = 10\pi$ (rad/s), and $\kappa_p = 0$, 1 and ∞. It is shown that the natural frequency ratio of the rotating FGM sandwich cylinders decreases with the increase of the thickness ratio, which implies the global stiffness of the cylinders increases with the increase of the thickness ratio, and then the rotation effect on the natural frequencies of these rotating FGM sandwich cylinders becomes insignificant.

Fig. 5 shows the least natural frequency parameters of a rotating FGM sandwich cylinder corresponding to the forward traveling waves for different vibration modes, in which $L/R = 20$, $R/$

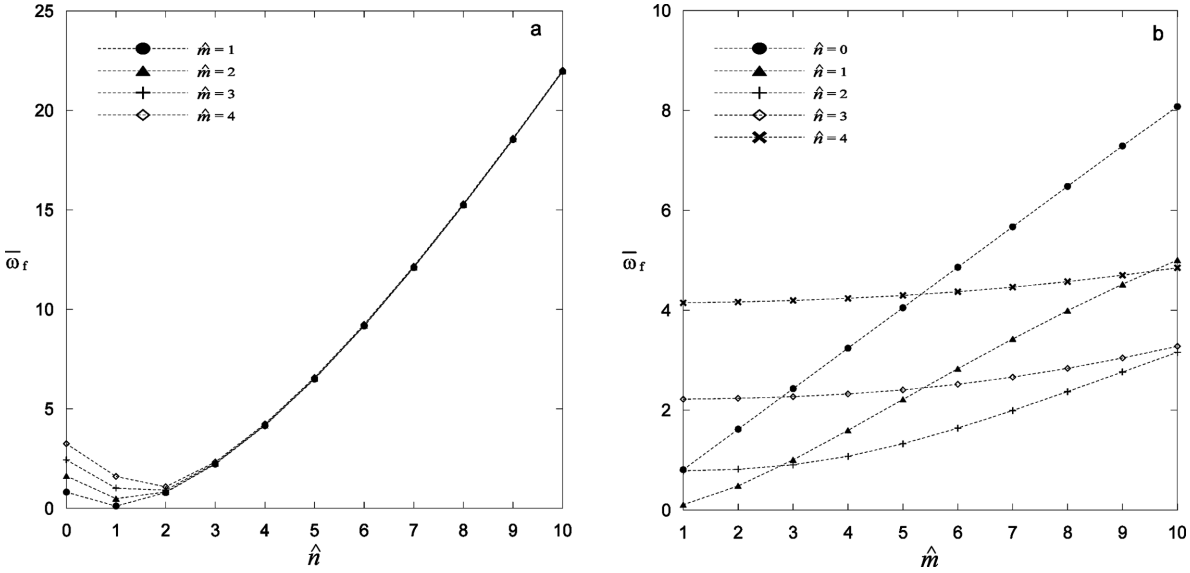

Fig. 5 Variations of the forward natural frequency parameter of a rotating FGM sandwich cylinder with the values of $\hat{m}$ and $\hat{n}$

$h = 10$, $R = 1$ m, $\Omega = 10\pi$ (rad/s), $h_1{:}h_2{:}h_3 = h/3{:}h/3{:}h/3$, $\kappa_p = 3$. It is seen in Figs. 5(a) and (b) that the least natural frequency parameters associated with the forward traveling waves first decrease with the increase of the full-circumferential wave number ($\hat{n}$), and then gradually increase again when the half-meridional wave number ($\hat{m}$) is fixed; while these monotonically increase with the increase of $\hat{m}$ when $\hat{n}$ is fixed. In addition, the fundamental frequency parameter in this studied case occurs in the vibration mode of ($\hat{m}$, $\hat{n}$) = (1, 1).

6. Conclusions

We present the exact 3D free vibration solutions of rotating simply-supported, multilayered FGM circular hollow cylinders using a modified Pagano method. The accuracy of the present solutions is found to be excellent by comparing them with the accurate solutions of rotating infinitely long isotropic cylinders, which are available in the literature. The convergence rate of the present method for an FGM sandwich cylinder is shown to be fast. In the illustrative examples, it is shown that for the rotating cylinders ($\Omega \neq 0$), pairs of natural frequency parameters corresponding to the backward and forward traveling modes are obtained, which are $\overline{\omega}_b$ and $\overline{\omega}_f$, respectively, while for the non-rotating cylinders ($\Omega = 0$), the repeated natural frequency parameters corresponding to the stationary vibration modes are obtained (i.e., $\overline{\omega}_b = \overline{\omega}_f$). A parametric study on the variations of the least natural frequency parameters corresponding to the backward and forward traveling waves with the assorted effects is also undertaken, such as the effects of thickness ratio, rotational speed, material-property gradient index, and vibration modes. It is noted that the Coriolis effect is much more significant than the centrifugal one on the natural frequency parameters of a rotating cylinder, and the rotation effect on the natural frequencies of a rotating thin cylinder is much more significant than on these of a thick one.

Acknowledgments

This work was supported by the National Science Council of Republic of China through Grant NSC 97-2211-E006-128-MY3.

References

Bryan, G.H. (1890), "On the beats in the vibrations of a revolving cylinder bell", *Proc. Cambridge Philos. Soc*., **7**, 101-111.

Carrera, E. (1999a), "Multilayered shell theories accounting for layerwise mixed description, Part 1: Governing equations", *AIAA J*., **37**(9), 1107-1116.

Carrera, E. (1999b), "Multilayered shell theories accounting for layerwise mixed description, Part 2: Numerical evaluations", *AIAA J*., 37(9), 1117-1124.

Carrera, E. (1999c), "A Reissner's mixed variational theorem applied to vibration analysis of multilayered shell", *J. Appl. Mech -T ASME*., **66**(1), 69-78.

Carrera, E. (2000a), "Single- vs multilayer plate modeling on the basis of Reissner's mixed theorem", *AIAA J*., **38**(2), 342-352.

Carrera, E. (2000b), "Assessment of mixed and classical theories on global and local response of multilayered orthotropic plates", *Compos. Struct*., **50**(2), 183-198.

Carrera, E. (2001), "Developments, ideas, and evaluations based upon Reissner's Mixed Variational Theorem in the modeling of multilayered plates and shells", *Appl. Mech. Rev*., **54**(4), 301-329.

Carrera, E. (2003), "Theories and finite elements for multilayered plates and shells: A unified compact formulation with numerical assessment and benchmarks", *Arch. Comput. Method. E*., **10**(3), 215-296.

Carrera, E., Brischetto, S., Cinefra, M. and Soave, M. (2010), "Refined and advanced models for multilayered plates and shells embedding functionally graded material layers", *Mech. Adv. Mater. Struc*., **17**, 603-621.

Chen, Y., Zhao, H.B., Shen, Z.P., Grieger, I. and Kröplin, B.H. (1993), "Vibrations of high speed rotating shells with calculations for cylindrical shells", *J. Sound Vib*., **160**(1), 137-160.

Cinefra, M., Belouettar, S., Soave, M. and Carrera, E. (2010), "Variable kinematic models applied to free-vibration analysis of functionally graded material shells", *Eur. J. Mech. A - Solid*., **29**, 1078-1087.

Di Taranto, R.A. and Lessen, M. (1964), "Coriolis acceleration effect on the vibration of a rotating thin-walled circular cylinder", *J. Appl. Mech -T ASME*., **31**(4), 700-701.

Guo, D., Zheng, Z. and Chu, F. (2002), "Vibration analysis of spinning cylindrical shells by finite element method", *Int. J. Soilds Struct*., **39**(3), 725-739.

Guo, D., Chu, F.L. and Zheng, Z.C. (2001), "The influence of rotation on vibration of a thick cylindrical shell", *J. Sound Vib*., **242**(3), 487-505.

Haddadpour, H., Mahmoudkhani, S. and Navazi, H.M., "Free vibration analysis of functionally graded cylindrical shells including thermal effects", *Thin. Wall. Struct*., **45**, 591-599.

Hill, R. (1965), "A self-consistent mechanics of composite materials", *J. Mech. Phys. Solids*, **13**(4), 213-222.

Hua, L. and Lam, K.Y. (2001), "Orthotropic influence on frequency characteristics of a rotating composite laminated conical shell by the generalized differential quadrature method", *Int. J. Solids Struct*., **38**(22-23), 3995-4015.

Huang, S.C. and Soedel, W. (1988), "On the forced vibration of simply supported rotating cylindrical shells", *J. Acoust. Soc. Am*., **84**(1), 275-284.

Huang, S.C. and Hsu, B.S. (1990), "Resonant phenomena of a rotating cylindrical shell subjected to a harmonic moving load", *J. Sound Vib*., **136**(2), 215-228.

Kadivar, M.H. and Samani, K. (2000), "Free vibration of rotating thick composite cylindrical shells using layerwise laminate theory", *Mech. Res. Commun*., **27**, 679-684.

Lam, K.Y. and Loy, C.T. (1994), "On vibrations of thin rotating laminated composite cylindrical shells", *Compos. Eng*., **4**(11), 1153-1167.

Lam, K.Y. and Loy, C.T. (1995a), "Free vibrations of a rotating multi-layered cylindrical shell", *Int. J. Solids*

Struct., **32**(5), 647-663.
Lam, K.Y. and Loy, C.T. (1995b), "Effects of boundary conditions on frequencies of a multi-layered cylindrical shell", *J. Sound Vib*., **188**(3), 363-384.
Lam, K.Y. and Loy, C.T. (1995c), "Analysis of rotating laminated cylindrical shells by different thin shell theories", *J. Sound Vib*., **186**(1), 23-35.
Lam, K.Y. and Loy, C.T. (1998), "Influence of boundary conditions for a thin laminated rotating cylindrical shell", *Compos. Struct*., **41**(3-4), 215-228.
Lam, K.Y. and Wu, Q. (1999), "Vibrations of thick rotating laminated composite cylindrical shells", *J. Sound Vib*., **225**(3), 483-501.
Leissa, A.W. (1973), *Vibration of Shells*, NASA SP-288. Washington.
Leissa, A.W. (1995), *Buckling and postbuckling theory for laminated composite plates*, (Eds., Turvey G.J. and Marshall IH), Buckling and Postbuckling of Composite Plates. Chapman and Hall, UK.
Padovan, J. (1973), "Natural frequencies of rotating prestressed cylinders", *J. Sound Vib*., **31**(4), 469-482.
Sepiani, H.A., Rastgoo, A., Ebrahimi, F. and Ghorbanpour Arani, A. (2010), "Vibration and buckling analysis of two-layered functionally graded cylindrical shell, considering the effects of transverse shear and rotary inertia", *Mater. Design*., **31**(3), 1063-1069.
Soedel, W. (1993), *Vibrations of Shells and Plates*, Marcel Dekker, Inc., New York.
Soldatos, K.P. and Hadjigeorgiou, V.P. (1990), "Three-dimensional solution of the free vibration problem of homogeneous isotropic cylindrical shells and panels", *J. Sound Vib*., **137**(3), 369-384.
Srinivasan, A.V. and Lauterbach, G.F. (1971), "Travelling waves in rotating cylindrical shells", *J. Eng. Industry*, **93**, 1229-1232.
Wang, H.M., Liu, C.B. and Ding, H.J. (2009), "Exact solution and transient behavior for torsional vibration of functionally graded finite hollow cylinders", *Acta Mech Sinica*, **25**(4), 555-563.
Wu, C.P., Chen, S.J. and Chiu, K.H. (2010), "Three-dimensional static behavior of functionally graded magnetoelectro-elastic plates using the modified Pagano method", *Mech. Res. Commun*., **37**(1), 54-60.
Wu, C.P. and Chiu, S.J. (2001), "Thermoelastic buckling of laminated composite conical shells", *J. Therm. Stresses*, **24**(9), 881-901.
Wu, C.P. and Chiu, S.J. (2002), "Thermally induced dynamic instability of laminated composite conical shells", *Int. J. Solids Struct*., **39**(11), 3001-3021.
Wu, C.P., Chiu, K.H. and Wang, Y.M. (2008), "A review on the three-dimensional analytical approaches of multilayered and functionally graded piezoelectric plates and shells", *Comput. Mater. Continua*, **8**, 93-132.
Wu, C.P. and Lu, Y.C. (2009), "A modified Pagano method for the 3D dynamic responses of functionally graded magneto-electro-elastic plates", *Compos. Struct*., **90**(3), 363-372.
Wu, C.P. and Tsai, Y.H. (2009), "Cylindrical bending vibration of functionally graded piezoelectric shells using the method of perturbation", *J. Eng. Math*., **63**(1), 95-119.
Yas, M. and Garmsiri, K., "Three-dimensional free vibration analysis of cylindrical shells with continuous grading reinforcement", *Steel Compos. Struct*., **10**, 349-360.
Ye, J. (2003), *Laminated Composite Plates and Shells-3D modelling*, Springer-Verlag, London, UK.
Zohar, A. and Aboudi, J. (1973), "The free vibrations of a thin circular finite rotating cylinder", *Int. J. Mech. Sci*., **15**(4), 269-278.

CC